

Optimal Vibration Control of Vehicle Engine-Body System using Haar Functions

Hamid Reza Karimi

Abstract: In this note a method of designing optimal vibration control based on Haar functions to control of bounce and pitch vibrations in engine-body vibration structure is presented. Utilizing properties of Haar functions, a computational method to find optimal vibration control for the engine-body system is developed. It is shown that the optimal state trajectories and optimal vibration control are calculated approximately by solving only algebraic equations instead of solving the Riccati differential equation. Simulation results are included to demonstrate the validity and applicability of the technique.

Keywords: Engine-body system, Haar function, optimal control, vibration control.

1. INTRODUCTION

Active control of sound and vibration has emerged as an important area of scientific and technological development in recent years. Developments in active control have allowed successful application of the concept in numerous industrial areas [1,2]. Recently, the noise and vibration of cars have become increasingly important. The predominant sources of interior noise in cars are engine and wheel vibrations, which propagate as structure-borne sound through the car body and finally radiate as airborne sound into the cabin [2,3-5]. A major comfort aspect is the transmission of engine-induced vibrations through powertrain mounts into the chassis (see Fig. 1). Engine and powertrain mounts are usually designed according to criteria that incorporate a trade-off between the isolation of the engine from the chassis and the restriction of engine movements. The engine mount is an efficient passive means to isolate the car chassis structure from the engine vibration. The passive means for isolation is efficient only in the high frequency range. However the vibration disturbance generated by the engine occurs mainly in the low frequency range [3,6-9]. These vibrations are result of the fuel explosion in the cylinder and the rotation of the different parts of the engine (see Fig. 2). The commercial use of engine and wheel mounts has

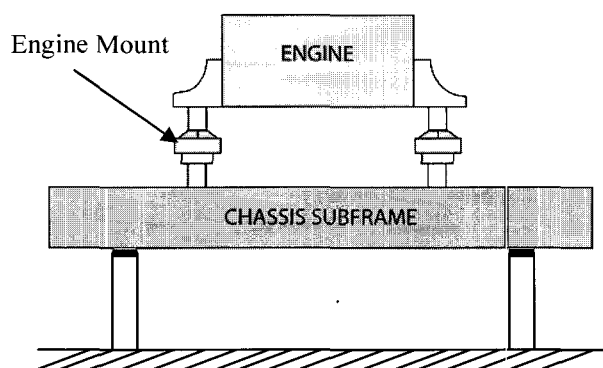


Fig. 1. Vehicle engine-body vibration system.

been impeded so far by technical problems. Compact and robust combinations of conventional rubber mounts with electrodynamically driven hydraulics have been constructed as active hydromounts for a wide frequency range [10], but the stroke and power required for cars at low frequencies cannot yet be fulfilled by active hydromounts of reasonable size [2].

A variety of control techniques, such as PID or Lead-Lag compensation, LQG/ H_2 , H_∞ , μ -synthesis and feedforward control have been used in active vibration systems [5,9,11-20]. The main characteristic of feedforward control is that information about the disturbance source is available and is usually realized with the Fx-LMS algorithms. However, the disturbance source is assumed to be unknown in feedback control, and then different strategies of feedback control for vibration attenuation of unknown disturbance exist ranging from classical methods to more advanced methods. Recently, the performance results obtained by feedback and feedforward controllers using Fx-LMS algorithms for vehicle engine-body vibration system were compared in [8,9].

Manuscript received August 7, 2005; revised April 24, 2006; accepted July 14, 2006. Recommended by Editorial Board member Kyongsu Yi under the direction of past Editor Keum-Shik Hong. This work was supported by the the Alexander von Humboldt-Foundation.

Hamid Reza Karimi is with the Control & Intelligent Processing Center, School of Electrical and Computer Engineering, University of Tehran, 14395-515, Tehran, Iran (e-mail: hrkarimi@ut.ac.ir).

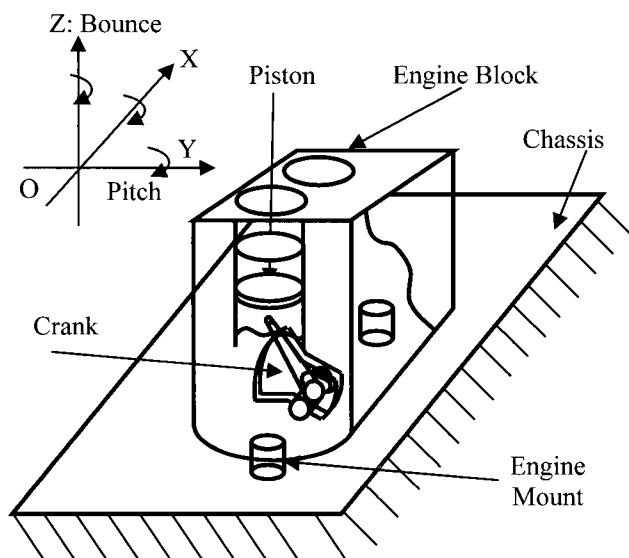


Fig. 2. Chassis excited by the engine vibration [8].

On the other hand, in the field of dynamic systems and control, orthogonal functions-based techniques of analysis, identification and control have received considerable attention in the recent years. This is evident from the vast amount of literature published over the last two decades [21,22]. The various systems of orthogonal functions may be classified into two categories. The first is the so-called piecewise constant basis functions to which the orthogonal systems of Haar functions (HFs) [23-25], block pulse functions [26] and Walsh functions [27] belong. These functions are constant over different segments within their intervals of definition and the functions and solutions represented using this class as basis is always staircase-approximated. The main characteristic of the piecewise constant basis functions is that these problems are reduced to those of solving a system of algebraic equations for the solution of problems described by differential equations. Thus, the solution, identification and optimisation procedure are either greatly reduced or much simplified accordingly [25,28-32]. Despite this, orthogonal polynomials such as Legendre, Laguerre, Chebyshev, Jacobi, Hermite along with sine-cosine functions were extensively applied to many areas of systems and control in the last decade [33-36]. The problems considered so far for orthogonal functions-based solutions include response analysis, optimal control, parameter estimation, model reduction, controller design, and state estimation. They have been applied to linear time-invariant and time-varying systems, nonlinear and distributed parameter systems, which include scaled systems, stiff systems, delay systems, singular systems and multivariable systems [22].

In the sequel, we apply the HFs to the finite-time optimal control problem of the second-order vehicle engine-body vibration system. Mathematical model of

the engine-body vibration structure is presented such the actuators and sensors used to investigate the optimal control are selected to be collocated. Moreover, the properties of HFs, Haar integral operational and Haar product operational matrices are given and are utilized to provide a systematic computational framework to find the optimal trajectory and finite-time optimal control of the vehicle engine-body vibration system approximately with respect to a quadratic cost function by solving only the linear algebraic equations instead of solving the differential equations. One of the main advantages is solving linear algebraic equations instead of solving nonlinear Riccati equation to optimize the control problem of the vehicle engine-body vibration system. Numerical results are presented to illustrate the applicability of the technique.

The rest of this paper is organized as follows. Section 2 introduces properties of the HFs. A dynamic model of the engine-body vibration structure is provided in Section 3. Algebraic solution of the engine-body system is given in Section 4 and development of optimal state trajectories and optimal vibration control by HFs are presented in Section 5. Simulation results of the vehicle engine-body vibration system are shown in Section 6 and finally the conclusion is discussed.

1.1. Notations

$A: r \times s$	matrix A with dimension $r \times s$;
I_r	identity matrix with dimension $r \times r$;
0_r	zero matrix with dimension $r \times r$;
$0_{r \times s}$	zero matrix with dimension $r \times s$;
\otimes	Kronecker product;
$vec(X)$	the vector obtained by putting matrix X into one column;
$tr(A)$	trace of matrix A .

2. HAAR FUNCTIONS

The original objective of the wavelet theory is to construct orthogonal bases of $L_2(\mathcal{R})$. These bases are constituted by translation and dilation of the same function $\psi(\cdot)$ and $\phi(\cdot)$, namely wavelet function and scaling function, respectively. These two functions generate a family of functions that can be used to break up or reconstruct a signal. To emphasize the 'marriage' involved in building this 'family' $\phi(\cdot)$ is sometimes called the 'father wavelet' and $\psi(\cdot)$, the 'mother wavelet' [21,37].

The oldest and most basic of the wavelet systems is named Haar wavelet, whose functions are given by

$$\psi_0(t) = 1, \quad t \in [0, 1), \quad (1)$$

$$\psi_1(t) = \begin{cases} 1, & \text{for } t \in \left[0, \frac{1}{2}\right), \\ -1, & \text{for } t \in \left[\frac{1}{2}, 1\right), \end{cases}$$

where $\phi(t) = \psi_0(t)$ and $\psi_i(t) = \psi_1(2^j t - k)$ for $i \geq 1$ with $i = 2^j + k$ for $j \geq 0$ and $0 \leq k < 2^j$. We can easily see that the $\psi_0(t)$ and $\psi_1(t)$ are compactly supported, they give a local description, at different scales j , of the considered function [25].

The finite series representation of any square integrable function $y(t)$ in terms of HFs in the interval $[0, 1)$, namely $\hat{y}(t)$, is given by

$$\hat{y}(t) = \sum_{i=0}^{m-1} a_i \psi_i(t) := a^T \Psi_m(t), \quad (2)$$

where $a := [a_0 \ a_1 \ \dots \ a_{m-1}]^T$ and $\Psi_m(t) := [\psi_0(t) \ \psi_1(t) \ \dots \ \psi_{m-1}(t)]^T$ for $m = 2^j$ and the Haar coefficients a_i are determined to minimize the mean integral square error $\varepsilon = \int_0^1 (y(t) - a^T \Psi_m(t))^2 dt$ and are given by

$$a_i = 2^j \int_0^1 y(t) \psi_i(t) dt. \quad (3)$$

Remark 1: The approximation error, $\Xi_y(m) := y(t) - \hat{y}(t)$, is depending on the resolution m and is approaching zero by increasing parameter of the resolution.

The integration of the vector $\Psi_m(t)$ can be approximated by

$$\int_0^t \Psi_m(r) dr = P_m \Psi_m(t), \quad (4)$$

where the matrix P_m represents the integral operator matrix for piecewise constant basis functions on the interval $[0, 1)$ at the resolution m . For HFs, the square matrix P_m satisfies the following recursive formula [24]:

$$P_m = \frac{1}{2m} \begin{bmatrix} 2mP_{\frac{m}{2}} & -H_{\frac{m}{2}} \\ H_{\frac{m}{2}}^{-1} & 0_{\frac{m}{2}} \end{bmatrix} \quad (5)$$

with $P_1 = \frac{1}{2}$ and $H_m^{-1} = \frac{1}{m} H_m^T \text{diag}(r)$ where the vector r is represented by $r := (1, 1, 2, 2, 4, 4, 4, 4, \dots, \underbrace{\left(\frac{m}{2}, \frac{m}{2}, \dots, \frac{m}{2}\right)^T}_{\left(\frac{m}{2}\right) \text{ elements}})$ for $m > 2$ and the matrix

H_m for $\frac{i}{m} \leq t_i < \frac{i+1}{m}$ is defined as

$$H_m = [\Psi_m(t_0), \Psi_m(t_1), \dots, \Psi_m(t_{m-1})]. \quad (6)$$

On the other hand, the product of two vectors $\Psi_m(t)$ is also evaluated as

$$R_m(t) := \Psi_m(t) \Psi_m^T(t), \quad (7)$$

where $R_m(t)$ satisfies the following recursive formula [24,28]

$$R_m(t) = \frac{1}{2m} \begin{bmatrix} R_{\frac{m}{2}}(t) & H_{\frac{m}{2}} \text{diag}(\Psi_b(t)) \\ (H_{\frac{m}{2}} \text{diag}(\Psi_b(t)))^T & \text{diag}(H_{\frac{m}{2}}^{-1} \Psi_a(t)) \end{bmatrix} \quad (8)$$

with $R_1(t) = \psi_0(t) \psi_0^T(t)$ and

$$\Psi_a(t) := [\psi_0(t), \psi_1(t), \dots, \psi_{\frac{m}{2}-1}(t)]^T = \Psi_{\frac{m}{2}}(t), \quad (9)$$

$$\Psi_b(t) := [\psi_{\frac{m}{2}}(t), \psi_{\frac{m}{2}+1}(t), \dots, \psi_{m-1}(t)]^T.$$

3. THE VEHICLE ENGINE-BODY SYSTEM

In this section a dynamic formulation of the characteristics of the vehicle engine-body vibration system is provided for vibration control design. A schematic diagram of the vehicle engine-body vibration structure is shown in Fig. 3, where the engine with mass M_e and inertia moment I_e is mounted in the body by the engine mounts k_e, c_e and the vehicle body with mass M_b and inertia moment I_b is supported by front and rear tires, each of which is modeled as a system consisting of a spring k_b and a damping device c_b . The front mount is the active mount, the output force of which can be controlled by an electric signal. The active mount consists of a main chamber where an oscillating mass (inertia mass) is moving up and down. The inertia mass is driven by an electro-magnetic force generated by a magnetic coil which is controlled by the input current.

In our study, only the bounce and pitch vibrations in the engine and body are considered. It is assumed that the actuator and sensor used to this control framework are selected to be collocated, since this arrangement is ideal to ensure the stability of the closed loop system for a slightly damped structure. Furthermore, the controller is tested for a single frequency signal, which is used to simulate the engine disturbance at particular frequency.

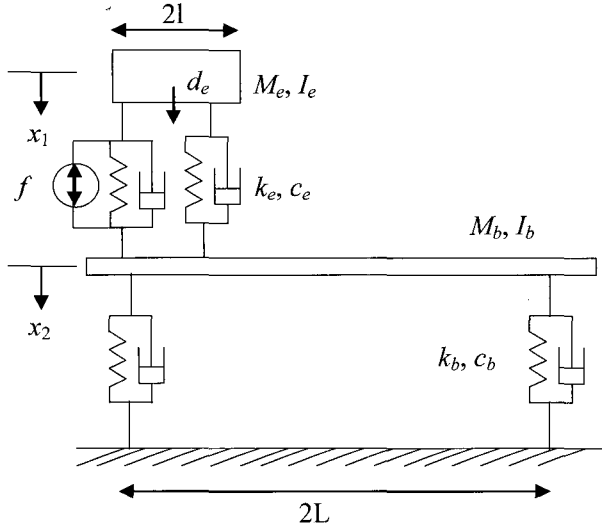


Fig. 3. The sketch of engine-body vibration system [9].

The derivation of the dynamic equations for a four degree-of-freedom vibration suspension model shown in Fig. 3 accordingly follows [9]:

$$\begin{aligned}
 M_e \ddot{x}_1 + 2c_e \dot{x}_1 + 2k_e x_1 - 2c_e \dot{x}_2 - 2k_e x_2 - 2(L-l)c_e \dot{x}_4 \\
 - 2(L-l)k_e x_4 &= f + d_e, \\
 M_b \ddot{x}_2 + 2(c_e + c_b) \dot{x}_2 + 2(k_e + k_b)x_2 - 2c_e \dot{x}_1 - 2k_e x_1 \\
 + 2(L-l)c_e \dot{x}_4 + 2(L-l)k_e x_4 &= -f, \\
 I_e \ddot{x}_3 + 2l^2 c_e \dot{x}_3 + 2l^2 k_e x_3 - 2l^2 c_e \dot{x}_4 - 2l^2 k_e x_4 &= lf, \\
 I_b \ddot{x}_4 + ((L^2 + (L-2l)^2)c_e + 2L^2 c_b) \dot{x}_4 + ((L^2 + (L-2l)^2)k_e \\
 + 2L^2 k_b)x_4 - 2l^2 c_e \dot{x}_3 - 2l^2 k_e x_3 - 2lc_e \dot{x}_1 - 2lk_e x_1 \\
 + 2(L-l)c_e \dot{x}_2 + 2(L-l)k_e x_2 &= -Lf,
 \end{aligned} \tag{10}$$

where

$f(t)$: input force, which is used as the active force to compensate the vibration transmitted to vehicle body (or to the chassis);

$d_e(t)$: engine disturbance, which can be the excitation, generated by the motion up/down of the different parts inside the engine;

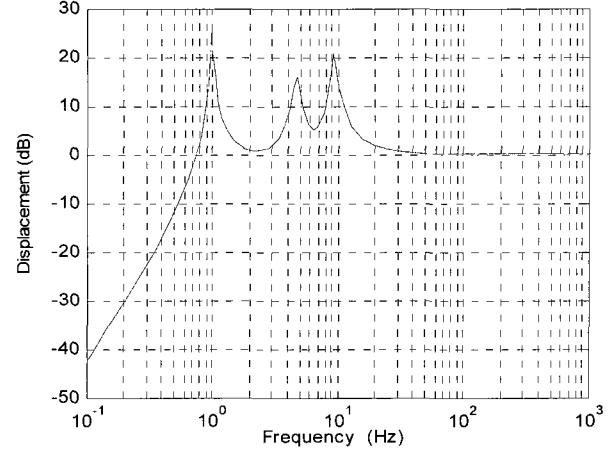
$x_1(t)$, $x_2(t)$, $x_3(t)$, $x_4(t)$: the bounces and pitches of the engine and body, respectively.

The state-space representation of the system (10) is

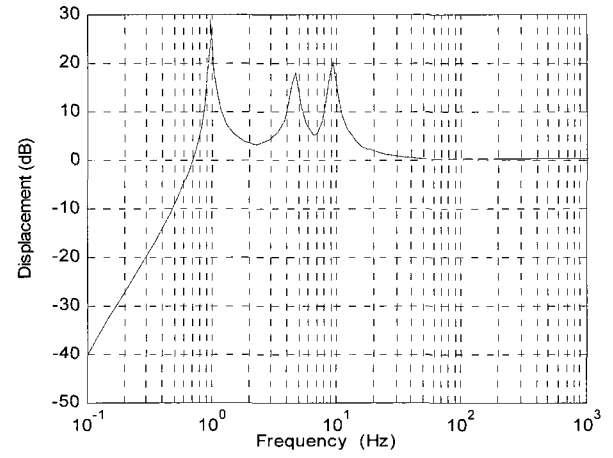
$$M\ddot{x}(t) + C\dot{x}(t) + Kx(t) = B_f f(t) + B_d d_e(t), \tag{11}$$

where the state-space matrices are defined as

$$M = \begin{bmatrix} M_e & 0 & 0 & 0 \\ 0 & M_b & 0 & 0 \\ 0 & 0 & I_e & 0 \\ 0 & 0 & 0 & I_b \end{bmatrix},$$



(a)



(b)

Fig. 4. Displacement of the chassis respect to $f(t)$ (a) and $d_e(t)$ (b).

$$C = \begin{bmatrix} 2c_e & -2c_e & 0 & -2(L-l)c_e \\ -2c_e & 2(c_e + c_b) & 0 & 2(L-l)c_e \\ 0 & 0 & 2l^2 c_e & -2l^2 c_e \\ -2lc_e & 2(L-l)c_e & -2l^2 c_e & 0 \end{bmatrix},$$

$$B_f = \begin{bmatrix} 1 \\ -1 \\ l \\ -L \end{bmatrix}, \quad B_d = \begin{bmatrix} 1 \\ 0 \\ 0 \\ 0 \end{bmatrix},$$

$$K = \begin{bmatrix} 2k_e & -2k_e & 0 & -2(L-l)k_e \\ -2k_e & 2(k_e + k_b) & 0 & 2(L-l)k_e \\ 0 & 0 & 2l^2 k_e & -2l^2 k_e \\ -2lk_e & 2(L-l)k_e & -2l^2 k_e & ((L^2 + (L-2l)^2)k_e + 2L^2 k_b) \end{bmatrix}.$$

Taking displacement of the chassis ($x_2(t)$) as an output then a comparison of the displacement

response respect to the input force $f(t)$ and the external disturbance $d_e(t)$ in the frequency range up to 1 KHz is depicted in Fig. 4(a) and 4(b). Three relevant modes occur around the frequencies 1, 5 and 9 Hz, respectively, which represent the dynamics of the main degrees of freedom (DOFs) of the system.

4. ALGEBRAIC SOLUTION OF SYSTEM EQUATIONS

The problem of solving the second-order differential equations of the engine-body system (10) in terms of the input control and exogenous disturbance is investigated using HFs and an appropriate algebraic equation is developed.

Based on definition of HFs on the time interval $[0, 1]$, we need to rescale the finite time interval $[0, T_f]$ into $[0, 1]$ by considering $t = T_f \sigma$; normalizing the system (11) with the time scale would be as follows

$$M\dot{x}(\sigma) + C\dot{x}(\sigma) + Kx(\sigma) = B_f f(\sigma) + B_d d_e(\sigma). \quad (12)$$

Now by integrating the system above in an interval $[0, \sigma]$, we obtain

$$\begin{aligned} M(\dot{x}(\sigma) - \dot{x}(0)) + T_f C(x(\sigma) - x(0)) + T_f^2 K \int_0^\sigma x(\tau) d\tau \\ = T_f^2 B_f \int_0^\sigma f(\tau) d\tau + T_f^2 B_d \int_0^\sigma d_e(\tau) d\tau. \end{aligned} \quad (13)$$

To avoid the differentiation of HFs, we take again the integration of (13) in the interval $[0, \sigma]$ as follows:

$$\begin{aligned} M(x(\sigma) - x(0)) + T_f C \int_0^\sigma x(\tau) d\tau + T_f^2 K \int_0^\sigma \int_0^\xi x(\tau) d\tau d\xi \\ = T_f^2 B_f \int_0^\sigma \int_0^\xi f(\tau) d\tau d\xi + T_f^2 B_d \int_0^\sigma \int_0^\xi d_e(\tau) d\tau d\xi \\ + \int_0^\sigma (M\dot{x}(0) + T_f Cx(0)) d\xi. \end{aligned} \quad (14)$$

By using the HF expansion (2), we express in the following the solution $x(\sigma)$, input force $f(\sigma)$ and engine disturbance $d_e(\sigma)$ in terms of HFs

$$\begin{aligned} x(\sigma) &= X\Psi_m(\sigma), \\ f(\sigma) &= F\Psi_m(\sigma), \\ d_e(\sigma) &= D_e\Psi_m(\sigma), \end{aligned} \quad (15)$$

where $X:4 \times m$, $F:1 \times m$ and $D_e:1 \times m$ denote the wavelet coefficients of $x(\sigma)$, $f(\sigma)$ and $D_e(\sigma)$, respectively. The initial conditions of $x(0)$ and $\dot{x}(0)$ are represented by $x(0) = X_0\Psi_m(\sigma)$ and $\dot{x}(0)$

$= \bar{X}_0\Psi_m(\sigma)$, where the matrices $X_0:4 \times m$ and $\bar{X}_0:4 \times m$ are defined as

$$\begin{aligned} X_0 &:= [x(0) \quad \underbrace{0_{4 \times 1} \quad \dots \quad 0_{4 \times 1}}_{(m-1)}], \\ \bar{X}_0 &:= [\dot{x}(0) \quad \underbrace{0_{4 \times 1} \quad \dots \quad 0_{4 \times 1}}_{(m-1)}]. \end{aligned} \quad (16)$$

Therefore, using the HF expansions (15), the relation (14) becomes

$$\begin{aligned} M(X - X_0)\Psi_m(\sigma) + T_f CX \int_0^\sigma \Psi_m(\tau) d\tau + T_f^2 KX \\ \times \int_0^\sigma \int_0^\xi \Psi_m(\tau) d\tau d\xi = T_f^2 B_f F \int_0^\sigma \int_0^\xi \Psi_m(\tau) d\tau d\xi + T_f^2 B_d D_e \\ \times \int_0^\sigma \int_0^\xi \Psi_m(\tau) d\tau d\xi + (M\bar{X}_0 + T_f CX_0) \int_0^\sigma \Psi_m(\xi) d\xi. \end{aligned} \quad (17)$$

Moreover, using the Haar integral operational matrix P_m in (4) and omitting $\Psi_m(\sigma)$ in both sides of (17), we have

$$\begin{aligned} M(X - X_0) + T_f CXP_m + T_f^2 KXP_m^2 = T_f^2 B_f FP_m^2 \\ + T_f^2 B_d D_e P_m^2 + (M\bar{X}_0 + T_f CX_0)P_m. \end{aligned} \quad (18)$$

For calculating the matrix X , we apply the operator $\text{vec}(\cdot)$ to (18) and according to the property of the Kronecker product in the Appendix A1, the following algebraic relation is obtained

$$\begin{aligned} (I_m \otimes M)(\text{vec}(X) - \text{vec}(X_0)) + T_f (P_m^T \otimes C)\text{vec}(X) \\ + T_f^2 (P_m^{2T} \otimes K)\text{vec}(X) = T_f^2 (P_m^{2T} \otimes B_f)\text{vec}(F) \\ + T_f^2 (P_m^{2T} \otimes B_d)\text{vec}(D_e) + T_f (P_m^T \otimes C)\text{vec}(X_0) \\ + (P_m^T \otimes M)\text{vec}(\bar{X}_0). \end{aligned} \quad (19)$$

Solving (19) for $\text{vec}(X)$ leads to

$$\begin{aligned} \text{vec}(X) = \Delta_1 \text{vec}(F) + \Delta_2 \text{vec}(D_e) \\ + \Delta_3 \text{vec}(X_0) + \Delta_4 \text{vec}(\bar{X}_0), \end{aligned} \quad (20)$$

where the matrices $\Delta_1:4m \times m$, $\Delta_2:4m \times m$, $\Delta_3:4m \times 4m$, and $\Delta_4:4m \times 4m$ are defined as

$$\begin{aligned} \Delta_1 &= T_f^2 (T_f (P_m^T \otimes C) \\ &\quad + T_f^2 (P_m^{2T} \otimes K) + I_m \otimes M)^{-1} (P_m^{2T} \otimes B_f), \\ \Delta_2 &= T_f^2 (T_f (P_m^T \otimes C) \\ &\quad + T_f^2 (P_m^{2T} \otimes K) + I_m \otimes M)^{-1} (P_m^{2T} \otimes B_d), \\ \Delta_3 &= (T_f (P_m^T \otimes C) + T_f^2 (P_m^{2T} \otimes K) + I_m \otimes M)^{-1} \\ &\quad \times (I_m \otimes M + T_f P_m^T \otimes C), \end{aligned} \quad (21)$$

$$\Delta_4 = (\Gamma_f (P_m^T \otimes C) + \Gamma_f^2 (P_m^{2T} \otimes K) + I_m \otimes M)^{-1} (P_m^T \otimes M).$$

Consequently, from (20), (21) and the properties of the Kronecker product, the solution of the system (11) is approximately

$$x(\sigma) = (\Psi_m^T(\sigma) \otimes I_4) \text{vec}(X). \quad (22)$$

5. OPTIMAL VIBRATION CONTROL DESIGN

The control objective is to find the optimal control $f(t)$ with respect to a quadratic cost functional approximately such acts as the active force to compensate the vibration transmitted to vehicle body (or the chassis). The quadratic cost functional weights the states and their derivatives with respect to time in the cost function as follows:

$$J = \frac{1}{2} x^T(\Gamma_f) S_1 x(\Gamma_f) + \frac{1}{2} \dot{x}^T(\Gamma_f) S_2 \dot{x}(\Gamma_f) + \frac{1}{2} \int_0^{\Gamma_f} (x^T(t) Q_1 x(t) + \dot{x}^T(t) Q_2 \dot{x}(t) + R f(t)^2) dt, \quad (23)$$

where $S_1: 4 \times 4$, $S_2: 4 \times 4$, $Q_1: 4 \times 4$ and $Q_2: 4 \times 4$ are positive-definite matrices and R is a positive scalar. We can rewrite the cost function (23) as follows:

$$J = \frac{1}{2} [x^T(\Gamma_f) \quad \dot{x}^T(\Gamma_f)] \tilde{S} \begin{bmatrix} x(\Gamma_f) \\ \dot{x}(\Gamma_f) \end{bmatrix} + \frac{1}{2} \int_0^{\Gamma_f} ([x^T(t) \quad \dot{x}^T(t)] \tilde{Q} \begin{bmatrix} x(t) \\ \dot{x}(t) \end{bmatrix} + R f(t)^2) dt, \quad (24)$$

where $\tilde{S} = \text{diag}(S_1, S_2)$ and $\tilde{Q} = \text{diag}(Q_1, Q_2)$.

Normalizing (24) with the time scale $t = \Gamma_f \sigma$ yields

$$J = \frac{1}{2} [x^T(1) \quad \Gamma_f^{-1} \dot{x}^T(1)] \tilde{S} \begin{bmatrix} x(1) \\ \Gamma_f^{-1} \dot{x}(1) \end{bmatrix} + \frac{\Gamma_f}{2} \times \int_0^1 ([x^T(\sigma) \quad \Gamma_f^{-1} \dot{x}^T(\sigma)] \tilde{Q} \begin{bmatrix} x(\sigma) \\ \Gamma_f^{-1} \dot{x}(\sigma) \end{bmatrix} + R f(\sigma)^2) d\sigma. \quad (25)$$

From (15) and the relation $\dot{x}(\sigma) = \bar{X} \Psi_m(\sigma)$, where $\bar{X}: 4 \times m$ denotes the wavelet coefficients of $\dot{x}(\sigma)$ after its expansion in terms of HFs, we read

$$\begin{bmatrix} x(\sigma) \\ \Gamma_f^{-1} \dot{x}(\sigma) \end{bmatrix} = \begin{bmatrix} X \\ \Gamma_f^{-1} \bar{X} \end{bmatrix} \Psi_m(\sigma) := X_{aug} \Psi_m(\sigma), \quad (26)$$

where $X_{aug} = \begin{bmatrix} X \\ \Gamma_f^{-1} \bar{X} \end{bmatrix}$ and

$$\text{vec}(X_{aug}) = \begin{bmatrix} \text{vec}^T(X) & \Gamma_f^{-1} \text{vec}^T(\bar{X}) \end{bmatrix}^T. \quad (27)$$

Remark 2: By substituting $\dot{x}(\sigma) = \bar{X} \Psi_m(\sigma)$ into $x(\sigma) - x(0) = \int_0^\sigma \dot{x}(t) dt$, we have:

$$X \Psi_m(\sigma) - X_0 \Psi_m(\sigma) = \int_0^\sigma \bar{X} \Psi_m(\tau) d\tau, \quad (28)$$

and using (4), we read $X - X_0 = \bar{X} P_m$. Then, by applying the operator of $\text{vec}(\cdot)$ and according to the properties of Kronecker product in Appendix A1, we obtain

$$\text{vec}(X) - \text{vec}(X_0) = (P_m^T \otimes I_n) \text{vec}(\bar{X}). \quad (29)$$

By substituting the definition (26) in (29) and using the properties of the operator $\text{tr}(\cdot)$ in Appendix A1, the cost function (25) is given by

$$J = \frac{1}{2} (\text{tr}(M_f X_{aug}^T \tilde{S} X_{aug})) + \frac{\Gamma_f}{2} \times (\text{tr}(M X_{aug}^T \tilde{Q} X_{aug}) + R \text{tr}(M F^T F)), \quad (30)$$

where the matrices $M_m: m \times m$ and $M_{mf}: m \times m$ are defined as $M_m := \int_0^1 \Psi_m(\sigma) \Psi_m^T(\sigma) d\sigma$ and $M_{mf} := \Psi_m(1) \Psi_m^T(1)$, respectively. Using the properties of the Kronecker product in Appendix A1, we can write (30) as

$$J = \frac{1}{2} (\text{vec}^T(X_{aug} M_{mf})(I_m \otimes \tilde{S}) \text{vec}(X_{aug})) + \frac{\Gamma_f}{2} (\text{vec}^T(X_{aug} M_m)(I_m \otimes \tilde{Q}) \text{vec}(X_{aug}) + R \text{vec}^T(F) M_m \text{vec}(F)) \quad (31)$$

or

$$J = \frac{1}{2} (\text{vec}^T(X_{aug}) \Pi_{m1} \text{vec}(X_{aug}) + \text{vec}^T(F) \Pi_{m2} \text{vec}(F)), \quad (32)$$

where the matrices $\Pi_{m1}: 8m \times 8m$ and $\Pi_{m2}: m \times m$ are defined as $\Pi_{m1} = M_f^T \otimes \tilde{S} + \Gamma_f (M^T \otimes \tilde{Q})$ and $\Pi_{m2} = R \Gamma_f M_m$, respectively.

It is clear that the cost function of $J(\cdot)$ is a

function of $\frac{i}{m} \leq \sigma_i < \frac{i+1}{m}$, then for finding the optimal control law, which minimizes the cost functional $J(\cdot)$, the following necessary condition should be satisfied

$$\frac{\partial J}{\partial \text{vec}(F)} = 0. \quad (33)$$

By considering $\text{vec}(X_{aug})$, which is a function of $\text{vec}(F)$, and using the properties of derivatives of inner product of Kronecker product in Appendix A2, we find

$$\begin{aligned} \frac{\partial J}{\partial \text{vec}(F)} = & \frac{1}{2} \left(\frac{\partial \text{vec}^T(X_{aug})}{\partial \text{vec}(F)} \frac{\partial}{\partial \text{vec}(X_{aug})} (\text{vec}^T(X_{aug}) \right. \\ & \times \Pi_{m1} \text{vec}(X_{aug})) \\ & \left. + \frac{\partial}{\partial \text{vec}(F)} (\text{vec}^T(F) \Pi_{m2} \text{vec}(F)) \right). \end{aligned} \quad (34)$$

To further investigate the relation (34), from Appendix A3 we obtain

$$\begin{aligned} \frac{\partial \text{vec}^T(X_{aug})}{\partial \text{vec}(F)} = & \frac{\partial}{\partial \text{vec}(F)} [(*) \quad (**)] \\ = & [\Delta_1^T \quad \Gamma_f^{-1} \Delta_1^T (P_m^{-1} \otimes I_4)], \end{aligned} \quad (35)$$

where

$$\begin{aligned} (*) = & \text{vec}^T(U) \Delta_1^T + \text{vec}^T(D_e) \Delta_2^T \\ & + \text{vec}^T(X_0) \Delta_3^T + \text{vec}^T(\bar{X}_0) \Delta_4^T, \\ (**) = & \Gamma_f^{-1} (P_m^{-1} \otimes I_4) (\Delta_1 \text{vec}(F) + \Delta_2 \text{vec}(D_e) \\ & + \Delta_3 \text{vec}(X_0) + \Delta_4 \text{vec}(\bar{X}_0) - \text{vec}(X_0)). \end{aligned}$$

Therefore, we find

$$\begin{aligned} \frac{\partial J}{\partial \text{vec}(F)} = & [\Delta_1^T \quad \Gamma_f^{-1} \Delta_1^T (P_m^{-1} \otimes I_4)] \Pi_{m1} \text{vec}(X_{aug}) \\ & + \Pi_{m2} \text{vec}(F). \end{aligned} \quad (36)$$

Then the wavelet coefficients of the optimal control law will be in vector form as

$$\begin{aligned} \text{vec}(F) = & -\Pi_{m2}^{-1} [\Delta_1^T \quad \Gamma_f^{-1} \Delta_1^T (P_m^{-1} \otimes I_4)] \Pi_{m1} \\ & \times \text{vec}(X_{aug}). \end{aligned} \quad (37)$$

Consequently, from (20), (27), (29), and (37) the optimal vectors of $\text{vec}(X)$ and $\text{vec}(F)$ are found, respectively, in the following forms

$$\text{vec}(X) = (I_{4m} + \Delta_1 (\Pi_{m2}^{-1} [\Delta_1^T \quad \Gamma_f^{-1} \Delta_1^T (P_m^{-1} \otimes I_4)] \Pi_{m1}$$

$$\begin{aligned} & \times \left[\begin{array}{c} I_{4m} \\ \Gamma_f^{-1} (P_m^T \otimes I_4)^{-1} \end{array} \right]^{-1} (\Delta_2 \text{vec}(D_e) + (\Delta_1 \Pi_{m2}^{-1} \\ & \times [\Delta_1^T \quad \Gamma_f^{-1} \Delta_1^T (P_m^{-1} \otimes I_4)] \Pi_{m1} \left[\begin{array}{c} 0_{4m} \\ \Gamma_f^{-1} (P_m^T \otimes I_4)^{-1} \end{array} \right] + \Delta_3) \\ & \times \text{vec}(X_0) + \Delta_4 \text{vec}(\bar{X}_0)), \end{aligned} \quad (38)$$

and

$$\begin{aligned} \text{vec}(F) = & -\Pi_{m2}^{-1} [\Delta_1^T \quad \Gamma_f^{-1} \Delta_1^T (P_m^{-1} \otimes I_4)] \Pi_{m1} \\ & \times \left\{ \left[\begin{array}{c} I_{4m} \\ \Gamma_f^{-1} (P_m^T \otimes I_4)^{-1} \end{array} \right] (I_{4m} + \Delta_1 \Pi_{m2}^{-1} \right. \\ & \times [\Delta_1^T \quad \Gamma_f^{-1} \Delta_1^T (P_m^{-1} \otimes I_4)] \Pi_{m1} \left[\begin{array}{c} I_{4m} \\ \Gamma_f^{-1} (P_m^T \otimes I_4)^{-1} \end{array} \right]^{-1} \\ & \times (\Delta_2 \text{vec}(D_e) + (\Delta_1 \Pi_{m2}^{-1} [\Delta_1^T \quad \Gamma_f^{-1} \Delta_1^T (P_m^{-1} \otimes I_4)] \Pi_{m1} \\ & \times \left[\begin{array}{c} 0_{4m} \\ \Gamma_f^{-1} (P_m^T \otimes I_4)^{-1} \end{array} \right] + \Delta_3) \text{vec}(X_0) + \Delta_4 \text{vec}(\bar{X}_0)) \\ & \left. - \left[\begin{array}{c} 0_{4m} \\ \Gamma_f^{-1} (P_m^T \otimes I_4)^{-1} \end{array} \right] \text{vec}(X_0) \right\}. \end{aligned} \quad (39)$$

Finally, the Haar function-based optimal trajectories and optimal control are obtained approximately from (22) and $f(t) = \Psi_m^T(t) \text{vec}(F)$.

Remark 3: According to the properties of HFs and Haar product operational matrix in the Section 2, the matrix M_m can be calculated from the following recursive formula:

$$M_m = \frac{1}{2m} \begin{bmatrix} M_{\frac{m}{2}} & H_{\frac{m}{2}} \text{diag}(\hat{\Psi}_b(t)) \\ (H_{\frac{m}{2}} \text{diag}(\hat{\Psi}_b(t)))^T & \text{diag}(H_{\frac{m}{2}}^{-1} \hat{\Psi}_a(t)) \end{bmatrix} \quad (40)$$

with $M_1(t) = 1$ and

$$\begin{cases} \hat{\Psi}_a(t) := \left[e_1 P_m \Psi_m(1), e_2 P_m \Psi_m(1), \dots, e_{\frac{m}{2}} P_m \Psi_m(1) \right]^T, \\ \hat{\Psi}_b(t) := \left[e_{\frac{m}{2}} P_m \Psi_m(1), e_{\frac{m}{2}+1} P_m \Psi_m(1), \dots, e_{m-1} P_m \Psi_m(1) \right]^T, \end{cases} \quad (41)$$

where $e_i = [0_{1 \times (i-1)}, 1, 0_{1 \times (m-i)}]$ for $i = 1, 2, \dots, m$.

Remark 4: Since the vector $\Psi_m(\sigma)$ is constant within each of the m time intervals, the approximated optimal trajectories (38) and optimal control (39) can be expressed as

$$x(t) = \sum_{i=1}^m G_i \text{vec}(X_0) + \sum_{i=1}^m \bar{G}_i \text{vec}(\bar{X}_0) + \sum_{i=1}^m \tilde{G}_i \text{vec}(D_e), \quad (42)$$

$$f(t) = -\left(\sum_{i=1}^m F_i \text{vec}(X_0) + \sum_{i=1}^m \bar{F}_i \text{vec}(\bar{X}_0) + \sum_{i=1}^m \tilde{F}_i \text{vec}(D_e)\right) \quad (43)$$

with constant matrices $G_i: 4 \times 4m$, $\bar{G}_i: 4 \times 4m$, $\tilde{G}_i: 4 \times m$, $F_i: 1 \times 4m$, $\bar{F}_i: 1 \times 4m$ and $\tilde{F}_i: 1 \times m$ within each of time intervals $\frac{i}{m} \leq \sigma_i < \frac{i+1}{m}$ for $i = 0, 1, \dots, (m-1)$.

Remark 5: This fact of constant coefficient matrices is a consequence of using piecewise constant basis functions like HFs or Walsh functions, and cannot be achieved with smooth function sets like Legendre or Laguerre polynomials. Compared to Walsh functions, the HFs have additional advantages in computational effort. Of course, more detailed investigations on using other basis functions than HFs would be of interest.

6. NUMERICAL RESULTS

The parameters of the vehicle engine-body vibration model, used for the design and simulation are given in Tables 1 and 2. The objective is to find the optimal states and optimal input force approximately using HFs at the finite time interval $[0, 3]$. Moreover, the matrices $S_1: 4 \times 4$, $S_2: 4 \times 4$, $Q_1: 4 \times 4$ and $Q_2: 4 \times 4$ and scalar R in the cost function (23) are chosen as $S_1 = S_2 = 0_4$, $Q_1 = \text{diag}(1, 2, 1, 1)$, $Q_2 = \text{diag}(0.1, 0.2, 0.1, 0.1)$ and

Table 1. The vehicle body parameter.

Parameters	Values
M_b	1000 kg
I_b	810 kg m ²
k_b	20000 N/m
c_b	300 N/m/s
L_b	2.5 m

Table 2. The engine parameters.

Parameters	Values
M_e	250 kg
I_e	8.10 kg m ²
k_e	200000 N/m
c_e	200 N/m/s
L_e	0.5 m

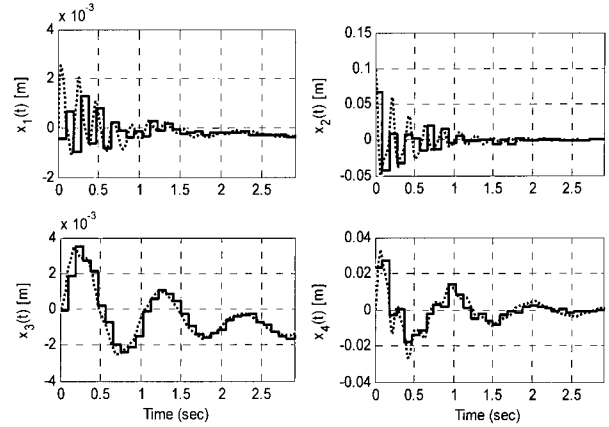


Fig. 5. Comparison of state trajectories found by HFs at resolution level $j = 5$ (solid line) and by analytic solution (dashed line).

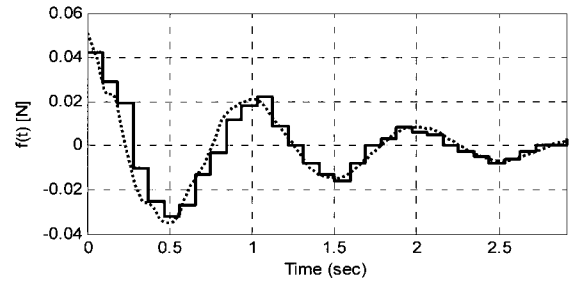


Fig. 6. Comparison of input force found by HFs at resolution level $j = 5$ (solid line) and by analytic solution (dashed line).

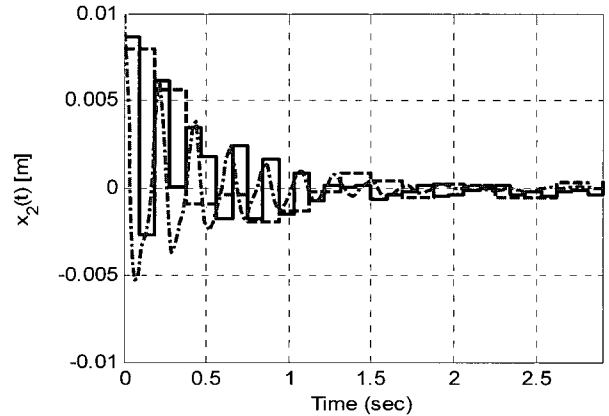


Fig. 7. Comparison of displacement of the chassis found by HFs at resolution level $j = 5$ (solid line), $j = 4$ (dashed line) and by analytic solution (dashed-dot line).

$R = 1$.

To show effect of the proposed optimal vibration control, the third mode of the low frequency range (see Fig. 4) is investigated and assumed to be excited by an external disturbance $d_e(t)$ as a $\text{Sin}(\cdot)$ function at the frequency 9Hz. Figs. 5 and 6 show

the comparison of states $x(\sigma)$ and optimal vibration control $f(\sigma)$ found by HFs at resolution level $j=5$ and the analytic solution found by solving the differential Riccati equation in Appendix A4, respectively. Figures show that the HFs can construct the vibration signals as well. Moreover, by increasing frequency of the external disturbance to 0.5KHz, the approximation displacement of the chassis ($x_2(t)$) at the resolution levels $j=4$ and 5 are plotted and compared to the analytic solution in Fig. 7. It is clear that by increasing the resolution level j the accuracy of the approximation can be improved as well.

Different from the analytic solution using the nonlinear Riccati equation, the approximate solutions (38) and (39) deliver both, control $f(t)$ and state trajectory $x(t)$ in one step, while mean square error can easily be improved by increasing the resolution level j .

7. CONCLUSION

This paper presented a method of designing optimal vibration control based on Haar functions (HFs) to control of bounce and pitch vibrations in engine-body vibration structure. Utilizing properties of HFs, a computational method to find optimal vibration control for the engine-body system was developed. It was shown that the optimal state trajectories and optimal vibration control are calculated approximately by solving only algebraic equations instead of solving the Riccati differential equation. The simulation results were included to illustrate the validity and applicability of the proposed technique.

APPENDIX A

A.1. Some properties of Kronecker product [38]

Let $A: p \times q$, $B: q \times r$, $C: r \times s$ and $D: q \times t$ be fixed matrices, then we have:

$$\text{vec}(ABC) = (C^T \otimes A)\text{vec}(B),$$

$$\text{tr}(ABC) = \text{vec}^T(A^T)(I_p \otimes B)\text{vec}(C),$$

$$\text{tr}(ABC) = \text{vec}^T(A^T)(I_p \otimes B)\text{vec}(C),$$

$$(A \otimes C)(D \otimes B) = AD \otimes CB.$$

A.2. Derivatives of inner products of Kronecker product [38]

Let $A: n \times n$ be fixed constants and $x: n \times 1$ be a vector of variables. Then, the following results can be established:

$$\frac{\partial(Ax)}{\partial x} = \text{vec}(A),$$

$$\frac{\partial(Ax)}{\partial x^T} = A,$$

$$\frac{\partial(x^T Ax)}{\partial x} = Ax + A^T x.$$

A.3. Chain rule for matrix derivatives using Kronecker product [38]

Let Z be a $p \times q$ matrix whose entries are a matrix function of the elements of $Y: s \times t$, where Y is a function of matrix $X: m \times n$. That is, $Z = H_1(Y)$, where $Y = H_2(X)$. The matrix of derivatives of Z with respect to X is given by

$$\frac{\partial Z}{\partial X} = \left\{ \frac{\partial \text{vec}^T(Y)}{\partial X} \otimes I_p \right\} \left\{ I_n \otimes \frac{\partial Z}{\partial \text{vec}(Y)} \right\}.$$

A.4. Analytic solution to optimal control problem

Taking $z_1(t) = x(t)$ and $z_2(t) = \dot{x}(t)$ yields an augmented model for the second-order linear system (11) as follows:

$$\begin{bmatrix} I & 0 \\ 0 & M \end{bmatrix} \dot{z}(t) + \begin{bmatrix} 0 & -I \\ K & C \end{bmatrix} z(t) = \begin{bmatrix} 0 \\ B_f \end{bmatrix} f(t) + \begin{bmatrix} 0 \\ B_d \end{bmatrix} d_e(t)$$

and the quadratic cost function (23) can be also represented by

$$J = \frac{1}{2} \int_0^{T_f} (z^T(t) \bar{Q} z(t) + f(t)^2) dt,$$

where $z(t) = [z_1^T(t) \ z_2^T(t)]^T$, $\bar{Q} = \text{diag}(Q_1, Q_2)$ and the matrices of S_1 and S_2 are assumed to be zero. We can solve the following Riccati differential equation [39]

$$\begin{aligned} \dot{K}(t) = & -K(t) \begin{bmatrix} 0 & -I \\ -M^{-1}K & -M^{-1}C \end{bmatrix} - \begin{bmatrix} 0 & -I \\ -M^{-1}K & -M^{-1}C \end{bmatrix}^T \\ & \times K(t) + R^{-1}K(t) \begin{bmatrix} 0 & 0 \\ 0 & M^{-1}(B_f B_f^T + B_d B_d^T) M^{-T} \end{bmatrix} \\ & \times K(t) - \bar{Q}, \end{aligned}$$

where $K(T_f) = 0$, then the exact solution to optimal control problem will be obtained as

$$f(t) = -R^{-1} \begin{bmatrix} 0 & 0 \\ M^{-1}B_f & M^{-1}B_d \end{bmatrix}^T K(t) z(t) := -L(t) z(t),$$

where the row vector $L(t)$ is named the optimal feedback gain.

REFERENCES

- [1] B. Riley and M. Bodie, "An adaptive strategy

- for vehicle vibration and noise cancellation,” *Proc. of CDC*, 1996.
- [2] O. Tokhi and S. Veres, *Active Sound and Vibration Control: Theory and Applications*, IEE Control Engineering Series 62, London, United Kingdom, 2002.
 - [3] H. J. Karkosch, F. Svaricek, R. Shoureshi, and J. L. Vance, “Automotive applications of active vibration control,” *Proc. of European Control Conference*, 2000.
 - [4] R. Krtolica and D. Hrovat, “Optimal active suspension control based on a half-car model,” *Proc. of the 29th CDC*, pp. 2238-2243, 1990.
 - [5] A. Preumont, *Vibration Control of Active Structures: An Introduction*, Kluwer Academic Publishers, 1997.
 - [6] S. J. Elliott and P. A. Nelson, “Active noise control,” *IEEE Signal Processing Magazine*, vol. 10, no. 4, pp. 12-35, October 1993.
 - [7] A. M. McDonald, S. J. Elliott, and M. A. Stokes, “Active noise and vibration control within the automobile,” *Proc. of Active Control of Sound and Vibration*, pp. 147-157, Tokyo 1991.
 - [8] B. Seba, N. Nedeljkovic, J. Paschedag, and B. Lohmann, “Feedback control and FX-LMS feedforward control for car engine vibration attenuation,” *Applied Acoustics*, vol. 66, pp. 277-296, 2005.
 - [9] J. Yang, Y. Suematsu, and Z. Kang, “Two-degree-of-freedom controller to reduce the vibration of vehicle engine-body system,” *IEEE Trans. on Control Systems Technology*, vol. 9, no. 2, pp. 295-304, March 2001.
 - [10] G. Kim and R. Singh, “A study of passive and adaptive hydraulic engine mount systems with emphasis on nonlinear characteristics,” *J. Sound and Vibration*, vol. 179, pp. 427-453, 1995.
 - [11] G. Aglietti, J. Stoustrup, E. Rogers, R. Langley, and S. Gabriel, “LTR control methodologies for micro vibrations,” *Proc. IEEE CCA*, Sept. 1998.
 - [12] T. Cao, L. Chen, F. He, and K. Sammut, “Active vibration absorber design via sliding mode control,” *Proc. of American Control Conference*, pp. 1637-1638, June 2000.
 - [13] A. Cavallo, G. Maria, and R. Setola, “A sliding manifold approach for vibration reduction of flexible systems,” *Automatica*, vol. 35, pp. 1689-1696, 1999.
 - [14] M. Hino, Z. Iwai, I. Mizumoto, and R. Kohzawa, “Active vibration control of a multi-degree-of-freedom structure by the use of robust decentralized simple adaptive control,” *Proc. of IEEE CCA*, pp. 922-927, September 1996.
 - [15] J. Hong and D. S. Bernstein, “Bode integral constraints, collocation and spill over in active noise and vibration control,” *IEEE Trans. on Control Systems Technology*, vol. 6, no. 1, pp. 111-120, 1998.
 - [16] J. W. Kamman and K. Naghshineh, “A comparison of open-loop feedforward and closed-loop methods for active noise control using volume velocity minimization,” *Applied Acoustics*, vol. 57, pp. 29-37, 1999.
 - [17] K. Nonami and S. Sivriogu, “Active vibration control using LMI-Based mixed H_2/H_∞ state and output feedback control with nonlinearity,” *Proc. of the 35th Conf. on Decision and Control*, pp. 161-166, Dec. 1996.
 - [18] R. Shoureshi, A. H. Chaghajardi, and M. Bell, “Hybrid adaptive robust structural vibration control,” *Proc. of American Control Conference*, pp. 1012-1016, June 1999.
 - [19] L. Sievers and A. Flotow, “Linear control design for active vibration isolation of narrow band disturbances,” *Proc. of the 27th IEEE Conf. on Decision and Control*, Texas, pp. 1032-1037, 1988.
 - [20] M. Weng, X. Lu, and D. Tumper, “Vibration control of flexible beams using sensor averaging and actuator averaging methods,” *IEEE Trans. on Control Systems Technology*, vol. 10, no. 4, pp. 568-577, July 2002.
 - [21] H. R. Karimi, B. Lohmann, B. Moshiri, and P. J. Maralani, “Wavelet-based identification and control design for a class of non-linear systems,” *Int. J. Wavelets, Multiresolution and Image Processing*, vol. 4, no. 1, pp. 213-226, 2006.
 - [22] A. Patra and G. P. Rao, *General Hybrid Orthogonal Functions and Their Applications in Systems and Control*, Springer-Verlag, London, 1996.
 - [23] C. F. Chen and C. H. Hsiao, “Haar wavelet method for solving lumped and distributed-parameter systems,” *IEE Proc. Control Theory Appl.*, vol. 144, no. 1, pp. 87-94, 1997.
 - [24] C. H. Hsiao and W. J. Wang, “State analysis and parameter estimation of bilinear systems via Haar wavelets,” *IEEE Trans. on Circuits and Systems I: Fundamental Theory and Applications*, vol. 47, no. 2, pp. 246-250, 2000.
 - [25] H. R. Karimi, B. Lohmann, P. J. Maralani, and B. Moshiri “A computational method for solving optimal control and parameter estimation of linear systems using Haar wavelets,” *Int. J. Computer Mathematics*, vol. 81, no. 9, pp. 1121-1132, 2004.
 - [26] G. P. Rao, *Piecewise Constant Orthogonal Functions and Their Application to Systems and Control*, Springer-Verlag, Berlin, Heidelberg, 1983.
 - [27] C. F. Chen and C. H. Hsiao, “A state-space approach to walsh series solution of linear systems,” *Int. J. System Sci.*, vol. 6, no. 9, pp. 833-858, 1965.

- [28] H. R. Karimi, "A computational method to optimal control problem of time-varying state-delayed systems by Haar wavelets," *Int. J. Computer Mathematics*, vol. 83, no. 2, pp. 235-246, 2006.
- [29] H. R. Karimi, P. J. Maralani, B. Moshiri, and B. Lohmann, "Numerically efficient approximations to the optimal control of linear singularly perturbed systems based on Haar wavelets," *Int. J. Computer Mathematics*, vol. 82, no. 4, pp. 495-507, April 2005.
- [30] H. R. Karimi, B. Moshiri, B. Lohmann, and P. J. Maralani, "Haar wavelet-based approach for optimal control of second-order linear systems in time domain," *J. of Dynamical and Control Systems*, vol. 11, no. 2, pp. 237-252, 2005.
- [31] H. R. Marzban and M. Razzaghi, "Solution of time-varying delay systems by hybrid functions," *Mathematics and Computers in Simulation*, vol. 64, pp. 597-607, 2004.
- [32] M. Ohkita and Y. Kobayashi, "An Application of rationalized Haar functions to solution of linear differential equations," *IEEE Trans. on Circuit and Systems*, vol. 9, pp. 853-862, 1986.
- [33] R. Y. Chang and M. L. Wang, "Legendre polynomials approximation to dynamical linear state-space equations with initial and boundary value conditions," *Int. J. Control*, vol. 40, pp. 215-232, 1984.
- [34] I. R. Horng and J. H. Chou, "Analysis, parameter estimation and optimal control of time-delay systems via Chebyshev series," *Int. J. Control*, vol. 41, pp. 1221-1234, 1985.
- [35] C. Hwang and Y. P. Shin, "Laguerre operational matrices for fractional calculus and applications," *Int. J. Control*, vol. 34, pp. 557-584, 1981.
- [36] M. Razzaghi and M. Razzaghi, "Fourier series direct method for variational problems," *Int. J. Control*, vol. 48, pp. 887-895, 1988.
- [37] C. S. Burrus, R. A. Gopinath, and H. Guo, *Introduction to Wavelets and Wavelet Transforms*, Prentice Hall, Upper Saddle River, New Jersey, 1998.
- [38] A. Graham, *Kronecker Products and Matrix Calculus with Applications*, Halsted Press, John Wiley and Sons, NY, 1981.
- [39] M. Athans and P. L. Flab, *Optimal Control*, McGraw-Hill, New York, 1966.



Hamid Reza Karimi was born 1976 in Iran. He received the B.Sc. degree in power systems engineering (1st. rank) from Sharif University of Technology in 1998 and the M.Sc. and Ph.D. degrees both in control systems engineering from University of Tehran in 2001 and 2005, respectively.

Currently, he is a Post-doctoral Research Fellow of the Alexander von Humboldt Foundation with both Technical University of Munich and University of Bremen. Dr. Karimi received the Distinguished Researcher Award from University of Tehran in 2001 and 2005. He also received the German Academic Awards (DAAD Award) in 2003 and 2004. Moreover, he received the Distinguished PhD Award of the Iranian president in 2005. Dr. Karimi's research interests are in the areas of Wavelets, nonlinear systems, robust optimal control, numerical mathematics, singularly perturbed systems and vibration control of flexible structures. He has written more than 60 technical papers in the journals and conferences.